Coded Excitation for Infrared Non-destructive Testing of Steel Materials

Rupla Naik Mude, Soma Sekhara Balaji Panda, Venkata Subbarao Ghali, Amarnath Muniyappa and Ravibabu Mulaveesala*

Infrared Imaging Laboratories(IRIL), PDPM
Indian Institute of Information Technology, Design and Manufacturing Jabalpur,
Dumna Airport Road, Khamaria, Jabalpur, Madhya Pradesh India 482005

ABSTRACT

Extensive use of steel materials in numerous applications necessitates reliable non destructive testing procedures for their thorough evaluation. Infrared thermography has been proved as a promising evaluation method for characterization of these materials due to its whole field, fast and remote inspection capabilities. But lower power distributed to high frequencies in pulsed thermography and long repetitive experimentation of lock-in thermography limits conventional thermographic methods, which demands an efficient processing methodology for detection of subsurface anomalies located at different depths with moderate peak power heat sources in limited span of experimentation time. This paper highlights the applicability of digitized frequency modulated thermal wave imaging for defect detection in mild steel materials and provides a theoretical insight for the proposed technique. In addition, detection capability of the techniques has been compared with conventional phase based approach by taking signal

Introduction

Infrared non destructive testing (IRNDT) has been widely used in numerous applications in various disciplines such as civil, mechanical, electronic and structural engineering for remote inspection of metals, semiconductors and composites. IRNDT involves mapping of the temperature over the test object and identification of subsurface anomalies in it. This method gained wide acceptance in various fields due to its full field, non-contact and remote inspection capabilities. It can be carried out by either of the two main possible approaches, namely passive and active. In passive approach inherent thermal response over the test object is monitored and used for defect

detection. Its inability of deeper defect detection due to insufficient thermal contrast limits its applicability. However, in active approach, its controlled heat stimulation and well supported processing methods, emerged as reliable qualitative and quantitative surface and subsurface defect detection. In active approach, the test object is activated by a controlled stimulation and temporal temperature distribution of the surface is captured using an IR camera either in reflection or in transmission mode. Further captured thermal history of the surface has been processed to reveal subsurface features. Various stimulation methods are in practice to obtain temperature contrast by generating thermal waves in the test sample. Among them at present, Pulsed Thermography (PT), Lock in Thermography (LT) and Pulse Phased Thermography (PPT) are predominantly used in numerous applications. Due to well supported image processing methods, simplicity of evaluation and rapid inspection makes PT popular among the remaining methods [1]. In PT, the specimen surface is activated by a photo thermal excitation using a flash lamp or halogen lamps by imposing a short duration high peak power pulsed stimulus and temporal evolution of the surface temperature is captured with an infrared (IR) camera. Temporal thermal contrast over the surface is used in localizing the defects underneath the object surface. However unavailability of high peak power sources, non uniform emissivity and non uniform heating over the surface may result in erroneous predictions using PT, which limits its applicability even though it is a quickest method of evaluation. Instead of instantaneous high peak power excitation used in PT, continuous wave thermography makes use of low peak powers for longer durations with preferred excitation methods which can improve penetration of thermal waves and provide better depth analysis. LT and recently introduced Frequency modulated thermal wave imaging (FMTWI)s are typical examples of continuous wave methods. LT generates thermal wave inside test object for a low frequency sinusoidal incident heat flux, whose frequency is chosen according to the thermal properties and thickness of the object. But mono frequency excitation may not better resolve the defects located at different depths and demands repetitive experimentation with a number of frequencies is time consuming in realistic applications. Further analysis is carried either by phase or by magnitude approaches. Merits of phase analysis being less sensitive to above mentioned problems enhanced its use over magnitude analysis [2]. In PPT, test object is stimulated similar to PT, but analysis is carried by the application of Fast Fourier Transform (FFT) over thermal profiles of each pixel and phase information corresponding to various frequency components is extracted [3]. These phase images are used for defect detection. In order to overcome the limitations of conventional thermal wave imaging techniques, in FMTWI a chirped stimulation of a suitable band of frequencies at moderate power is imposed over the test object [4]. It provides an excellent depth resolution with contained band of frequencies in a single experimentation cycle unlike LT and at moderate powers unlike PT, by capturing the advantages of both of them. In order to impose more energy and simplify the generation of excitation by retaining the advantages of FMTWI, a digitized version of FMTWI (DFMTWI) has been used [5]. This paper presents a novel physical insight based on mathematical analysis of the thermal waves generated by DFMTWI.

Due to extensive use of steel samples in numerous fields, capability of the proposed technique has been experimentally investigated using a mild steel sample containing flat bottom holes.

Theory

Thermal waves of DFMTWI

In Active thermography, thermal behavior of the test object has been studied by providing a controlled stimulus of known parameters. Imposed energy over the test object, warms up infinitely thin layer over the surface and initiates a similar thermal disturbance. Thermal conductivity of the material facilitates the propagation of this thermal disturbance, which can be treated as a thermal wave, into the interiors of the object. In case of thermally homogeneous substances, this thermal diffusion uniformly modulates the temperature over the entire surface, Where as in the presence of defects, temperature contrast has been observed over the object surface due to thermal inhomogeneity. This section provides a theoretical outlook of the temperature evolution over the surface caused by the propagating thermal waves generated by the proposed method and focuses on its depth resolving capability.

Theoretical analysis of the surface temperature evolution due to thermal waves has been carried out by the application of one dimensional heat equation to the homogenous, isotropic and semi infinite media, in the absence of any heat sink or source. The 1D heat equation is given by

$$\frac{\partial^2 T(x,t)}{\partial x^2} = \frac{1}{\alpha}\frac{\partial T(x,t)}{\partial t} \tag{1}$$

Where $T(x,t)$ is the temperature, α is the thermal diffusivity. The space coordinate is x, and t is time. The solution for $T(x,t)$ is obtained by applying the boundary conditions at the sample surfaces $x=0$ and $x=d$, where surface at d is the surface opposite to the irradiated one at $x=0$. Assume a digitized linear frequency modulated surface heating caused by an incident modulated heat flux of peak power Q over the sample, given by

$$Q(x=0,t)=Q_0\left[\frac{2}{\pi}\sum_{k=-\infty}^{\infty}(-1)^k\frac{1}{2k+1}e^{j\phi}\right] \tag{2}$$

Here $\phi = 2\pi(2k+1)\left[ft+\frac{Bt^2}{2\tau}\right]$ and

B is the bandwidth, r is the duration, f is centre frequency and t is the instantaneous time of the digitized frequency modulated signal. The digitized linear frequency modulated temperature T is obtained by the imposed excitation is given by

$$T(x=0,t)=T_\infty+T_0\left[\frac{2}{\pi}\sum_{k=-\infty}^{\infty}(-1)^k\left(\frac{1}{2k+1}\right)e^{j\phi}\right] \tag{3}$$

Assuming ambient temperature $T_x=0$ and considering only the dynamic variations in temperature results in

$$T(x=0,t)=T_\infty+T_0\left[\frac{2}{\pi}\sum_{k=-\infty}^{\infty}(-1)^k\left(\frac{1}{2k+1}\right)e^{j\phi}\right] \tag{4}$$

On applying the above said boundary conditions the expression for *T(x,t)* may now be written in terms of real and imaginary parts,

$$T(x,t)=T_0\, e^{-x\sqrt{\frac{2\left(f+\frac{Bt}{\tau}\right)\sum_{k=-\infty}^{\infty}(-1)^k e^{2\pi j(2k+1)\left(f+\frac{Bt^2}{2\tau}\right)}}{\alpha g(t)}}}\frac{2}{\pi}\sum_{k=-\infty}^{\infty}(-1)^k\frac{1}{2k+1}e^{j\left(\phi-x\sqrt{\frac{\xi_1}{2}}\right)} \tag{5}$$

$$g(t)=\frac{2}{\pi}\sum_{k=-\infty}^{\infty}(-1)^k\frac{1}{2k+1}e^{j\phi}$$

$$\xi_1=\frac{4j\left(f+\frac{Bt}{\tau}\right)}{j\alpha\, g(t)}\sum_{k=-\infty}^{\infty}(-1)^k e^{2\pi j(2k+1)\left(ft+\frac{Bt^2}{2\tau}\right)}$$

This clearly represents the resultant temperature evolution obtained by the wave like propagation of the heat flow into the sample. From the above expression the thermal diffusion length can be written as follows

$$\mu=\sqrt{\frac{\alpha\, g(t)}{2\left(f+\frac{Bt}{\tau}\right)\sum_{k=-\infty}^{\infty}(-1)^k e^{2\pi j(2k+1)\left(ft+\frac{Bt^2}{2\tau}\right)}}} \tag{6}$$

Hence knowledge of the thermal properties of the sample and modulation frequency of the incident excitation enables the thermal diffusion length within the sample, which is a measure of the probing depth of thermal waves in the sample. It is clear from Eq.6 that in DFMTWI, time dependant change in diffusion length provides depth scanning in a single experimentation cycle unlike LT.

Need for DFMTWI

The digitized chirp reduces the complexity of the signal generation by taking switch over at zero crossings of the analog chirp. As the energy of a digitized chirp is twice to that of the analog chirp, it can probe more energy into the test object and facilitates generation of thermal waves with enhanced amplitude. Further more, it increases the bandwidth of the excitation by retaining the original bandwidth of its analog counterpart along with higher order harmonics and enhances its depth resolution capability.

Pulse compression for DFMTWI

Pulse compression concentrates [6,7] the imposed energy into a pseudo pulse which improves the detection capability, provides better resolution and facilitates usage of low peak power sources.

Compression processing between two similar profiles integrates the energy at some time instant depending on the delay between them. In thermal imaging, obtained temporal thermal response from each pixel is not only attenuated but also delayed depending on the depth of the underneath thermal inhomogeneity. Delay between these thermal profiles with respect to the chosen reference provides an analogous delay in the corresponding compressed profile. Compression can be achieved either through convolution or correlation. In present context, correlation based matched filter analysis has been adopted for defect detection. The delay of the cross correlated thermal response is used for detection and quantitative analysis of anomalies. Cross correlation of the received signal with the impulse response of the matched filter is given by

$$g(\tau)= \int_{-\infty}^{\infty} s(t)\ h(\tau+t)\ dt \qquad (7)$$

Usually can be any chosen reference profile similar to the response profiles s(t) with a finite attenuation and delay. As a result, the long duration (D sec) signal is compressed to a duration of '1/ B ', governed by the bandwidth (Hz) of the waveform. The ratio of the time durations of transmitted and compressed signals is called the compression ratio.

Results and Discussions

Applicability for Defect detection and comparison of processing methods

Applicability of the proposed excitation method is experimentally tested on a mild steel sample as shown in Fig. 1.

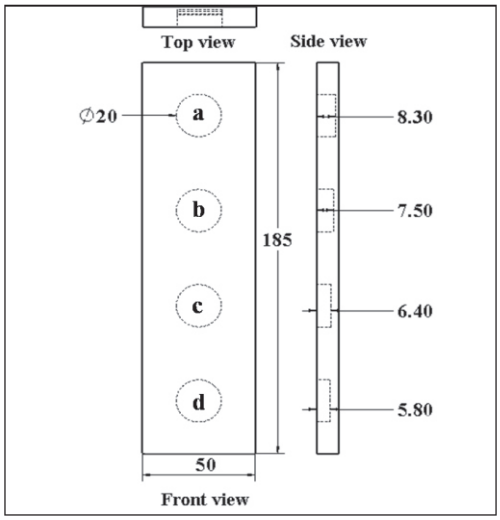

Fig. 1: Layout of the experimental mild steel sample with 4 flat bottom holes. (All the dimensions are in mm and depths represented from the bottom)

The experimental mild steel specimen of 9.9 mm thickness contains circular flat bottom holes of diameter 20mm, kept at different depths from the front surface are considered as defects shown in Fig. 1

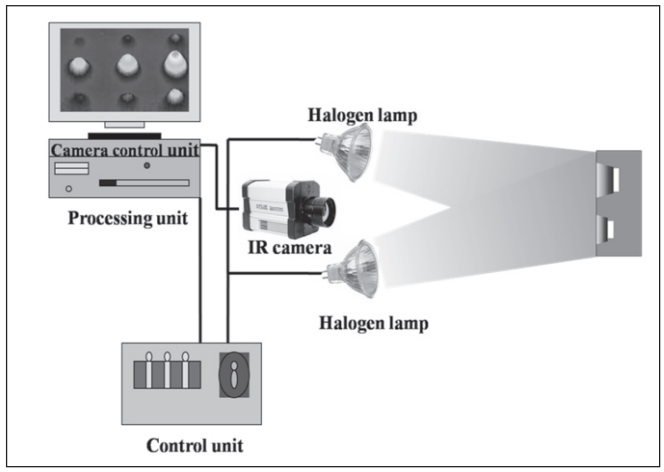

Fig. 2: Experimental setup for DFMTWI

Experimental arrangement adopted for carrying out proposed 'DFMTWI' is as shown in Fig. 2. DFMTWI signal (square chirp) of duration 100 sec and frequencies swept from 0.01 to 0.1Hz is generated to drive the halogen lamp sources via a source control. Two halogen lamps of 1kW each are employed to excite the sample. Temporal temperature map over the sample has been recorded by the infrared camera at a frame rate of 25 Hz.

Further processing on the experimental data has been carried to reveal subsurface defects using correlation based pulse compression and conventional phase based approaches. In order to carry out the data processing, temporal thermal profiles of each pixel have been extracted from the captured data. Mean increased temperature during the transient heating has been removed from each profile using a polynomial fit and the proposed processing methods (correlation and phase) are applied over these mean removed profiles.

In phase based analysis, Fast Fourier Transform (FFT) is applied over to the mean removed temporal thermal profile of each pixel and phase information has been extracted. Phase images are obtained by arranging the extracted phase information. Phase contrast generated due to the presence of inhomogeneity is observed in phase image of a particular frequency can be used for identification of the defect location. In correlation based approach, mean removed temporal thermal profiles of each pixel is cross correlated with the chosen reference, which results in a pseudo pulse centered about a delayed instant depending on the group delay between the profiles. Delay between these correlated profiles of defective and non defective pixels contributes for a normalized correlation coefficient difference. Normalized correlation coefficient contrast at a particular instant of time is used to identify the defective regions.

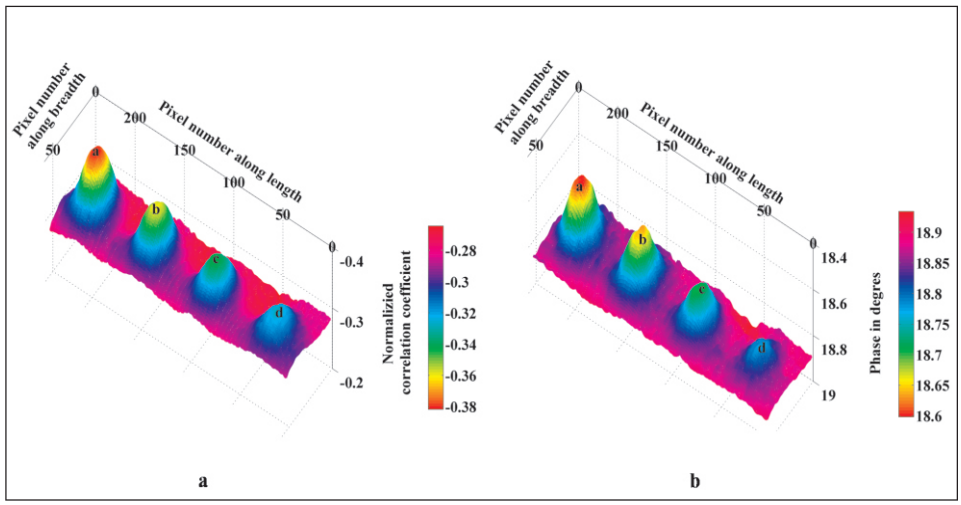

Fig. 3: Experimentally obtained images for mild steel sample; (a) Correlation image obtained at 9.56 s, (b). Phase image obtained at 0.0854 Hz (phase contrast in degrees).

Fig. 3 illustrates the detectability of DFMTWI for mild steel sample using correlation and phase based processing approaches [8,9] and visibility was quantified using SNR. Correlation image obtained at a delayed instant of 9.56 s, as shown in Fig. 3(a), exhibited overall detection ability better than the best phase image, Fig. 3(b), obtained at a frequency of 0.0854 Hz.

In particular an enhanced detection is obtained with deeper defect (d) in correlation processing at a delayed instant of 9.56 s than the best phase image as shown in Fig. 3. Results illustrated the ability of the correlation analysis over conventional phase based analysis in improving the detectability due to its energy concentration and noise reluctance. Detectability has been compared by taking SNR as a measure of contrast, which is obtained by considering the defective and non defective regions for a defect is computed as,

$$\text{SNR} = \frac{\text{Mean of the defective area} - \text{Mean of the non defective area}}{\text{Standard deviation of the non defective area}} \quad (8)$$

SNRs of the defects obtained from different approaches has been shown in Fig. 4. SNR values illustrated in Fig. 4 clearly represent the enhanced visibility obtained from correlation processing for the proposed DFMTWI. From Fig. 4, quite a large difference (10.4148 db) in SNR value with deeper defect (d) has been found between correlation and phase images of mild steel specimen.

Correlation delay vs. defect depth

Temporal thermal profiles from the center of the defects are not only attenuated but also delayed depending on the depth of the defect underneath the surface.

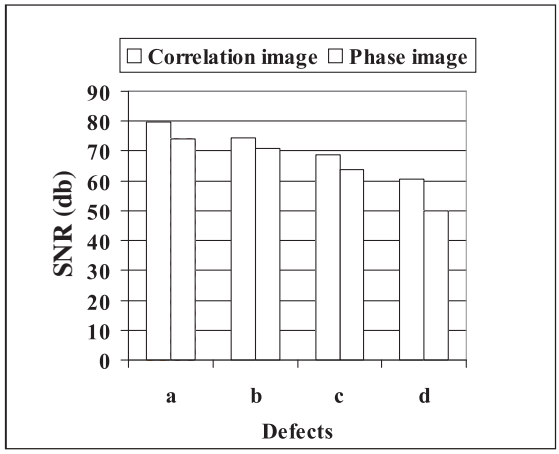

Fig. 4: SNR of the defects in various processing approaches for mild steel sample.

This is clear from the Fig. 5 correlation coefficient values of defects with respect to sound can be considered as a measure of the defect depth from normalized correlation coefficient value, which is acquired from correlation of sound with defects. Fig. 6(a) shows the obtained experimental relation between the normalized correlation coefficient and defect depth. The values obtained from correlation profiles is fitted ($y = ax^2 + bx + c$, where y is normalized correlation coefficient and x is depth and $a = -9.288 \times 10^{-1}$, and $b = -4.0333 \times 10^{-3}$) as shown.

In addition to earlier approach, time delay at zero crossing has also been considered for estimation of defect depth. Fig. 6(b) illustrates the empirical relation between the zero crossing correlation delay and defect depth. The data obtained from the delayed zero crossing correlation profiles are fitted in to $t = ae^{-tx} + ce^{-dx}$ ($a = 0.4265$, $b = 4.603 \times 10^{-4}$, $c = -2.427 \times 10^{-4}$ and $d = 1.919$) where t is the delay and x is the depth of the defect.

Conclusion

A theoretical basis has been provided for the proposed DFMTWI. Results obtained from the experimental data with the mild steel specimen clearly show the capability of the correlation based pulse compression approach over the conventional phase based approach for defect detection.

References

1. N. P. Avdeldis, and D. P., Almond, in Infrared Physics & Technology 45, (2004),p-103.
2. G. Busse, D. Wu, and W. Karpen, J.Appl. Phys., 71, (1992), 3962.
3. X. Maldague and S. Marinetti, J. Appl. Phys. 79, (1996), 2694
4. R. Mulaveesala and S.Tuli, Appl. Phys. Lett. 89, (2006) 191913.
5. R. Mulaveesala, R. and S. Tuli, S, Materials Evaluation 64,(2005), 1046
6. R. Mulaveesala, V. Jyani Somayajulu, V. and S. Pushpraj, Rev. Sci. Instrum. 79, (2008) 094901
7. N. Tabatabaei, N. and A. Mandelis, Rev. Sci. Instrum, 80 (2009), 034902.
8. V.S. Ghali, N. Jonnalagadda, and R. Mulaveesala, IEEE Sensors Journal, 9 (2009), 832.
9. V.S. Ghali, and R. Mulaveesala, Insight, 52, (2010), 475.

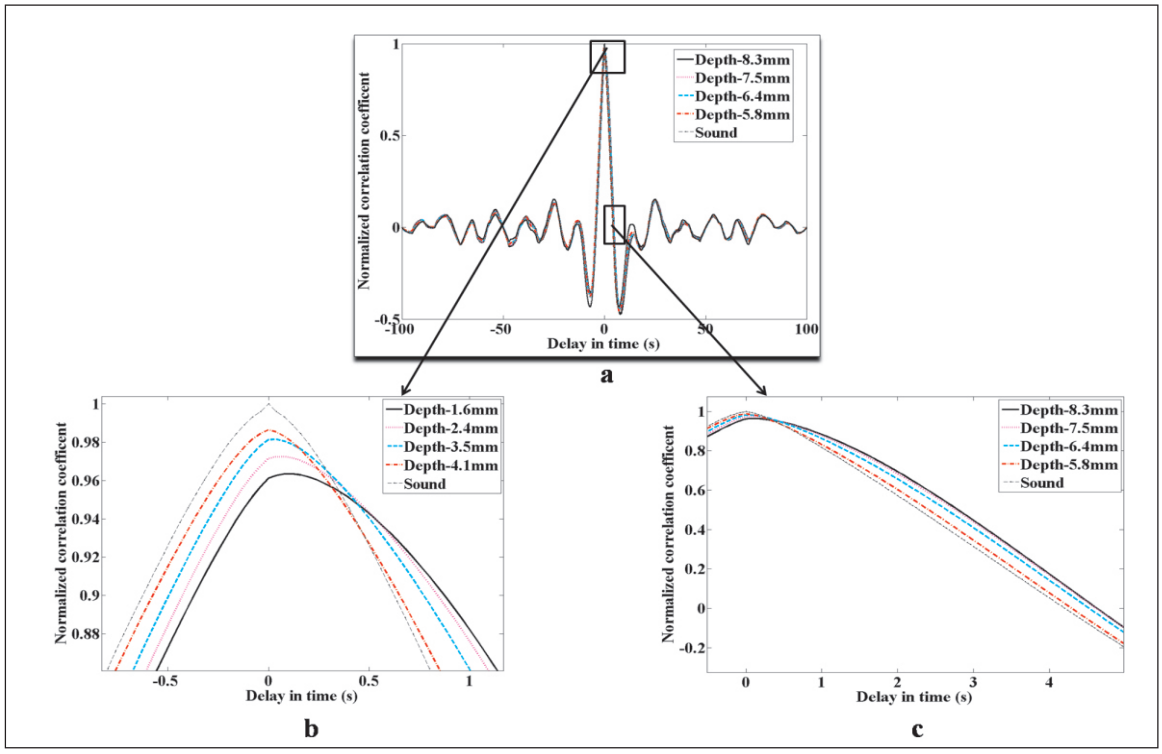

Fig. 5: Normalized correlation peaks obtained from experiment for different defect depths.

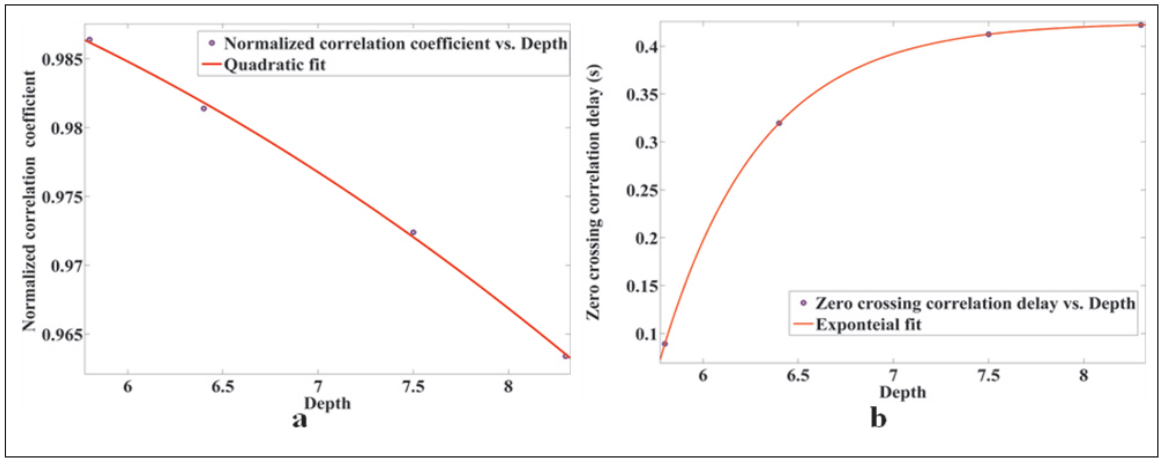

Fig. 6: (a) Normalized correlation coefficient for different defect depths, (b) Zero crossing correlation delay (s) for different defect depths